Report

Current Biology

Amphibian mucus triggers a developmental transition in the frog-killing chytrid fungus

Highlights

- *Bd* encysts within 5 min of exposure to amphibian mucus or purified mucin
- Mucin-induced encystation includes ciliary retraction and *de novo* cell wall assembly
- Triggered encystation requires surface adhesion but not gene expression
- Calcium flux appears necessary and sufficient to induce encystation

Authors

Kristyn A. Robinson, Sarah M. Prostak, Evan H. Campbell Grant, Lillian K. Fritz-Laylin

Correspondence

lfritzlaylin@umass.edu

In brief

The chytrid fungus *Batrachochytrium dendrobatidis* (*Bd*) causes a skin infection that is decimating global amphibian populations. Robinson et al. report here that exposure to amphibian mucus causes *Bd* to rapidly transition from its dispersal to its growth form and identify key molecular requirements of this essential developmental transition.

Robinson et al., 2022, Current Biology *32*, 2765–2771
June 20, 2022
https://doi.org/10.1016/j.cub.2022.04.006

CellPress

Current Biology

CellPress
OPEN ACCESS

Report

Amphibian mucus triggers a developmental transition in the frog-killing chytrid fungus

Kristyn A. Robinson,[1] Sarah M. Prostak,[1] Evan H. Campbell Grant,[2] and Lillian K. Fritz-Laylin[1,3,4,*]
[1]University of Massachusetts, Department of Biology, 611 N. Pleasant Street, Amherst, MA 01003, USA
[2]United States Geological Survey, Patuxent Wildlife Research Center, 1 Migratory Way, Turners Falls, MA 01376, USA
[3]Twitter: @fritzlaylin
[4]Lead contact
*Correspondence: lfritzlaylin@umass.edu
https://doi.org/10.1016/j.cub.2022.04.006

SUMMARY

The frog-killing chytrid fungus *Batrachochytrium dendrobatidis* (*Bd*) is decimating amphibian populations around the world.[1–4] *Bd* has a biphasic life cycle, alternating between motile zoospores that disperse within aquatic environments and sessile sporangia that grow within the mucus-coated skin of amphibians.[5,6] Zoospores lack cell walls and swim rapidly through aquatic environments using a posterior flagellum and crawl across solid surfaces using actin structures similar to those of human cells.[7,8] *Bd* transitions from this motile dispersal form to its reproductive form by absorbing its flagellum, rearranging its actin cytoskeleton, and rapidly building a chitin-based cell wall—a process called "encystation."[5–7] The resulting sporangium increases in volume by two or three orders of magnitude while undergoing rounds of mitosis without cytokinesis to form a large ceonocyte. The sporangium then cellurizes by dividing its cytoplasm into dozens of new zoospores. After exiting the sporangium through a discharge tube onto the amphibian skin, daughter zoospores can then reinfect the same individual or find a new host.[5] Although encystation is critical to *Bd* growth, whether and how this developmental transition is triggered by external signals was previously unknown. We discovered that exposure to amphibian mucus triggers rapid and reproducible encystation within minutes. This response can be recapitulated with purified mucin, the bulk component of mucus, but not by similarly viscous methylcellulose or simple sugars. Mucin-induced encystation does not require gene expression but does require surface adhesion, calcium signaling, and modulation of the actin cytoskeleton. Mucus-induced encystation may represent a key mechanism for synchronizing *Bd* development with the arrival at the host.

RESULTS AND DISCUSSION

Bd zoospores encyst upon exposure to amphibian mucus and purified mucin

Batrachochytrium dendrobatidis (*Bd*) takes 3–4 days to complete its life cycle in pure culture, with zoospores taking up to 24 h to encyst.[9,10] If *Bd* actively seeks out a host, it must do so prior to encystation as afterward it can no longer crawl or swim.[6,7] Moreover, if *Bd* retains its motility after finding a host, it risks leaving a productive growth site. This means that triggered encystation upon arrival at an amphibian host could increase colonization rates. Because *Bd* grows in amphibian skin that is coated in mucus[5,11]—a complex mixture of antimicrobial peptides, small molecules, and microbes that are embedded in a viscous matrix of heavily glycosylated proteins called mucins[12–15]—we hypothesized that amphibian skin mucus could trigger encystation.

To test our hypothesis that mucus induces *Bd* encystation, we imaged zoospores before, during, and for 10 min following exposure to mucus isolated from wild green frogs (*Lithobates clamitans*). Because *Bd* zoospores rapidly swim out of the field of view, we adhered both mucus-treated and control zoospores to the imaging plane by coating the coverglass with the lectin concanavalin-A (ConA), a common surface coating for cell adhesion.[7,8] Within minutes of exposure to amphibian mucus, the mucus-treated *Bd* zoospores retracted their flagella and become round—two clear signs of encystation (Figure 1A, left; Video S1). To quantify this encystation response, we counted the number of cells with retracted flagella over time and found that 54.2% of mucus-treated cells encysted between 2 and 9 min after exposure (mean time: 5.7 ± 0.3 min), whereas only 3.0% of the control cells that were treated with buffer alone encysted during the same time period (Figure 1A, right).

We next tested if the encystation response could be recapitulated by exposure to mucins, a diverse family of heavily glycosylated proteins that form the viscous, bulk component of mucus.[13–15] We added 10 mg/mL of commercially purified porcine stomach mucins to adhered cells and saw a similar response (Figures 1B–1D). To confirm that the cells were encysting, we fixed zoospores 5 min after mucin exposure and stained them for cell wall material (calcofluor white), flagella (tubulin tracker), and actin (fluorescent phalloidin). Although control cells lacked cell walls and had an actin cortex, pseudopods, and a posterior flagellum, mucin-exposed cells displayed all three

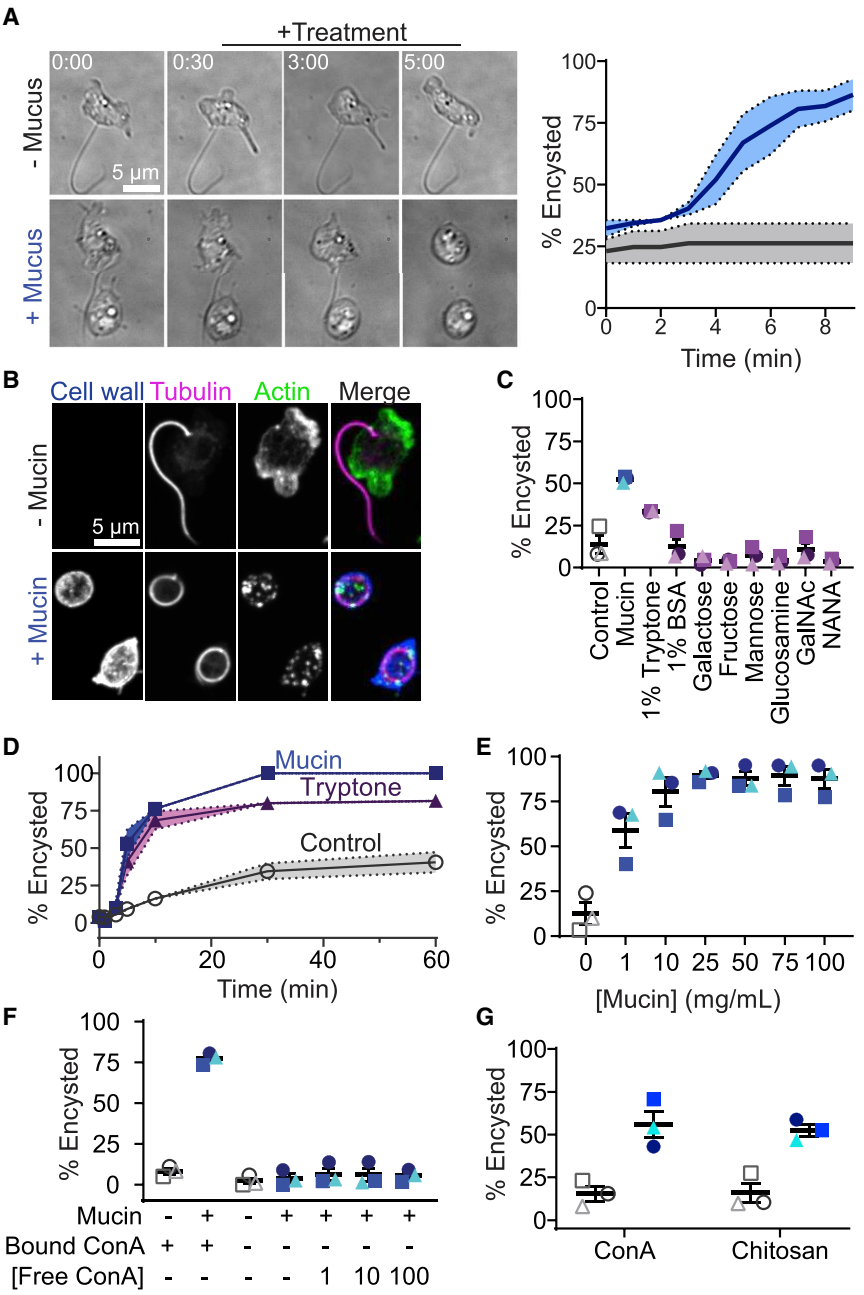

Figure 1. Adherent *Bd* zoospores encyst upon exposure to amphibian mucus or purified mucin

(A) Images of live *Bd* zoospores exposed to buffer (control) or amphibian mucus (min:s). Right: accumulation of encysted cells after mucus exposure. Mean and standard error of two replicates using mucus from individual frogs shown.

(B) Cells exposed to buffer (control) or 10 mg/mL purified mucin stained for cell wall (calcofluor white), flagella (tubulin tracker), and actin (phalloidin).

(C) Percent cells encysted after 5 min of indicated treatment.

(D) Time course showing percent cells encysted after treatment with buffer, 10 mg/mL mucin, or 1% tryptone. The mean of three independent biological replicates is plotted at each time point with shading to show SEM.

(E) Percent cells encysted after 5 min of treatment with the indicated concentration of mucin.

(F) Percent cells encysted 5 min after addition of mucin or buffer (control) while adhered to a ConA-coated surface (bound ConA) or in suspension with the indicated concentration of ConA in solution.

(G) Percent cells encysted after 5 min exposure to mucin or buffer (control) when adhered to ConA (left) or chitosan (right).

(C–G) Open shapes represent control; filled shapes represent mucin (blue) or alternative treatment (purple). Means and standard errors of three independent biological replicates are shown. Significance (bold font for $p \leq 0.05$) tested by ordinary one-way ANOVA (C and F) or unpaired t tests (G). See also Figure S1, Data S1, and Video S1.

hallmarks of encystation: actin patches, a retracted axoneme, and a cell wall (Figure 1B).[5–7] We quantified the percentage of cells that had each hallmark over time and found that although only 40.6% ± 6.9% of control cells encyst after 1 h, 100% ± 0% of mucin-exposed cells are encysted within 30 min of mucin exposure (Figure 1D). We saw equivalent results using mucin purified from either porcine stomach or bovine submaxillary gland (Figure S1B).

The glycosyl chains of mucins are typically 2–12 monosaccharides long and include galactose, fructose, mannose, glucosamine (GlcN), N-acetylgalactosamine (GalNAc), N-acetylglucosamine (GlcNAC), and sialic acids, particularly N-acetyl-neuraminic acid (NANA).[16] We tested each of these constituents in our encystation assay, as well as a variety of other simple sugars, and found no response after 5 min (Figures 1C and S1C), although it remains possible that a combination of these compounds could induce encystation. To determine whether *Bd* may be responding to a physical property of hydrated mucin, we tested similarly viscous methylcellulose[17] and saw no effect (Figure S1C). We also tested altering the osmotic pressure of the extracellular environment by adding various concentrations of sorbitol and again saw no effect (Figure S1C). We next wondered if *Bd* is responding to the protein in mucin and tested its response to another protein, bovine serum albumin (BSA), and again observed no response (Figure 1C). Because *Bd* encysts in culture medium, we also tested the response to 1% tryptone—the media in which we grow *Bd*—and found that this treatment induced a partial encystation response (33.3% ± 0.3%, $p = 0.0034$; Figure 1C). Given the complex composition of tryptone—an enzymatic digest of casein—it remains unclear which molecular signature triggers tryptone-induced encystation.

To measure the speed of the encystation response to mucin and tryptone, we conducted an encystation time course

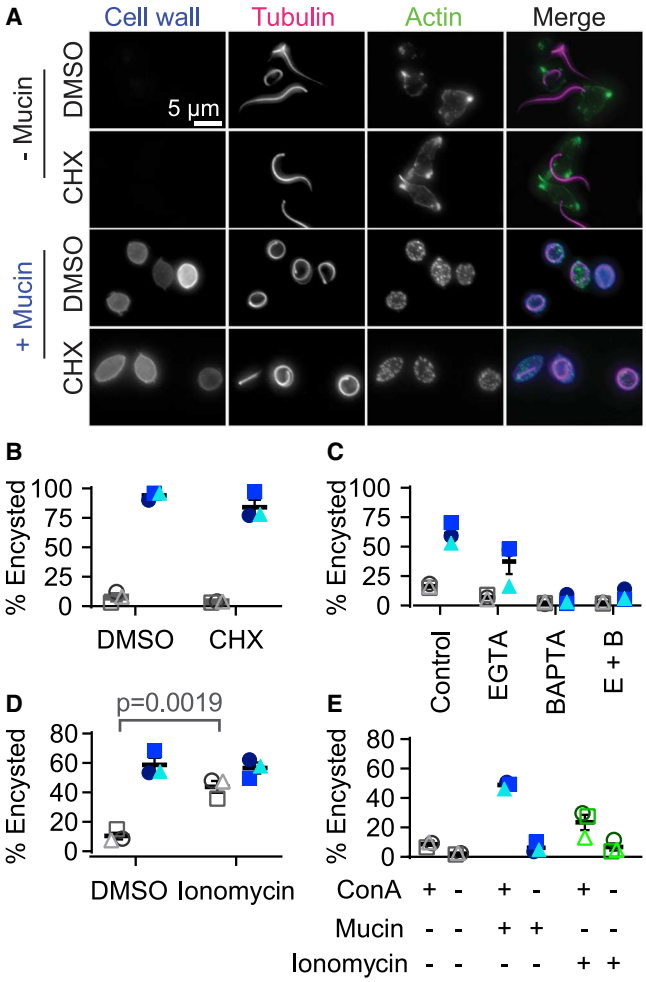

Figure 2. Encystation is driven by calcium signaling, not protein translation

(A) Cells exposed to buffer (control) or 10 mg/mL mucin and DMSO or cycloheximide (CHX) stained for cell wall (calcofluor white), flagella (tubulin tracker), and actin (phalloidin).

(B) Percent cells encysted after DMSO (left) or cycloheximide (CHX; right) treatment upon exposure to control buffer or mucin.

(C and D) Percent encysted cells treated with the indicated (C) calcium chelator, (D) ionophore, or (C and D) DMSO carrier control 5 min after adding mucin or control buffer while adhered to a ConA-coated surface.

(E) Percent cells encysted after addition of control buffer, mucin, or ionomycin while adhered to a ConA-coated surface or in suspension. Filled shapes represent mucin (blue), open shapes represent the control (gray) and ionomycin (green), and each shape corresponds to data from three independent biological replicates.

Significance (bold font or $p \leq 0.05$) tested by unpaired t test (B and D) or ordinary one-way ANOVA (C and E). Means and SEM of three biological replicates are shown.

See also Figure S2 and Data S1.

between 1 and 60 min after exposure to buffer (control), 10 mg/mL mucin, or 10 mg/mL tryptone (1%) (Figure 1D). We found that although all (100% ± 0%) of mucin-treated cells encysted after 60 min, fewer tryptone-treated cells encysted (81.5% ± 4.1%). The kinetics of the response also differed slightly; mucin-treated cells reached half maximum encystation by 3 min, whereas tryptone took 5 min. We next measured the dose response of mucin- and tryptone-induced encystation at 5 min. We found that although the encystation response to both treatments were dose dependent, the maximum response to tryptone resulted in the encystation of only 18.7% ± 3.4% of cells (Figure S1D, 10 mg/mL tryptone), whereas mucin could induce encystation in 89.6% ± 2.0% (Figure 1E, 25 mg/mL mucin). This maximum response to tryptone is less than our initial experiments and is emblematic of the month-to-month variability we observe in induced encystation that may be a result of long-term selection for robust growth in tryptone media. Given the speed and near completeness of mucin-induced encystation, we also tested whether the kinetics of mucin-induced encystation were also concentration dependent and found that treatment with 100 mg/mL mucin decreased the time to half maximum encystation to less than a minute (Figure S1E). Because *Bd* encysted within 5 min of treatment with frog mucus and previous estimates of mucin concentrations of 10–20 mg/mL in the skin mucus of aquatic animals,[18] we chose a 5-min exposure of 10 mg/mL mucin as our standard for the remaining experiments.

We next tested whether surface adhesion was necessary for mucin-induced encystation by exposing zoospores to mucin in the presence and absence of a ConA-coated surface and found that only cells adhered to ConA-coated surfaces encysted in response to mucin ($p \leq 0.0001$; Figure 1F), even when we added various concentrations of ConA in suspension. To determine whether mucin-induced encystation is specific to ConA-mediated adhesion, we first needed to identify other surfaces to which *Bd* could attach. By testing a panel of other possible surface coatings (Figure S1F), we found that *Bd* adheres equally well to chitosan (a polymer derived from chitin[19]) and only slightly to polyethyleneimine (another commonly used cell adhesive[20]) and mucin. We confirmed that *Bd* tightly binds ConA and chitosan using interference reflection microscopy to visualize the region of the cell in close contact with the coverslip[21] (Figure S1G). *Bd*'s adhesion to ConA and chitosan may be an active process as heat-killed cells fail to adhere to either substrate (Figure S1F). We next compared the ability of ConA and chitosan to facilitate mucin-induced encystation and found that both surface treatments worked equivalently ($p = 0.0112$ and $p = 0.0055$, respectively; Figure 1G). Together, these data indicate that mucus-induced encystation can be recapitulated by purified mucin, but not simple sugars, and requires surface adhesion.

Mucin-induced encystation is calcium mediated and does not require gene expression

Previous reports suggested that encystation of *Bd* may not require gene expression.[22] To test whether mucin-induced encystation involves gene expression, we treated cells with 150 μg/mL of cycloheximide (CHX) for 10 min prior to encystation to block global mRNA translation. Although this concentration (533 μM) is sufficient to disrupt downstream growth and development (Figure S2A), cells were still able to robustly encyst upon exposure to mucin ($p = 0.0002$; Figures 2A and 2B), indicating that mucin-induced cell wall assembly requires no new protein synthesis. This is similar to encystation in other chytrid species.[23,24]

Given its speed, we hypothesized that calcium signaling may be coordinating the events that comprise encystation. We therefore pretreated ConA adhered zoospores with the calcium

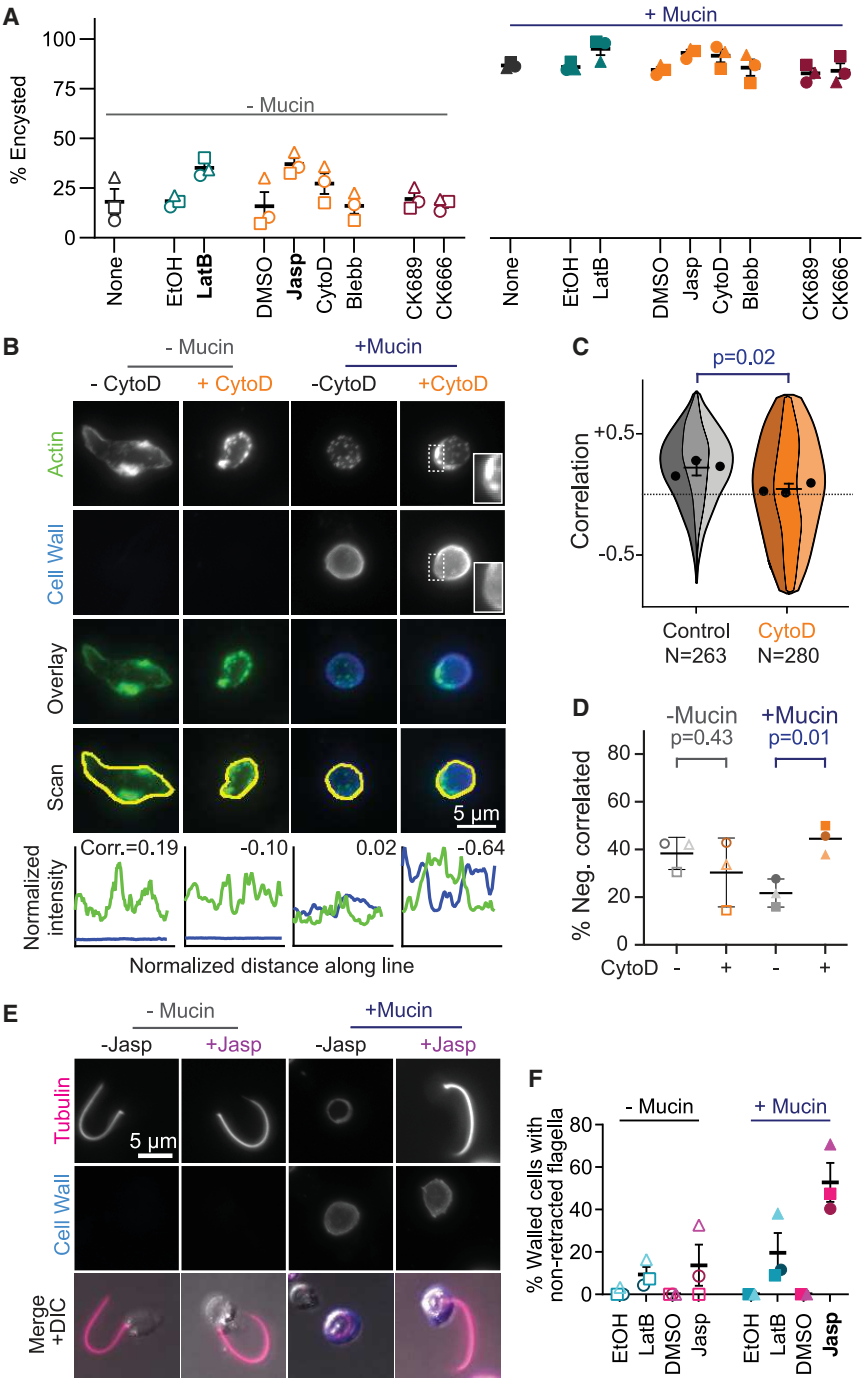

Figure 3. Actin cortex disassembly is associated with cell wall assembly

(A) Percent cells encysted when exposed to buffer (left) or mucin (right) after indicated treatment.

(B) Representative cells treated with DMSO or Cytochalasin D (CytoD), exposed to buffer or mucin, and stained for actin (phalloidin) and cell wall (calcofluor white). Graphs show normalized fluorescence intensity of actin (green) and cell wall (blue) along yellow lines with associated Pearson's correlation coefficient.

(C) SuperViolin plot[28] of correlation coefficients of actin and cell wall intensity in mucin-exposed cells treated with DMSO (gray) or CytoD (orange). N = number of cells quantified by line scans; p values calculated using unpaired t test, shades indicate independent replicates.

(D) Percent cells with negatively correlated actin and cell wall intensities upon exposure to buffer or mucin after treatment with DMSO or CytoD.

(E) Representative cells treated with DMSO or jasplakinolide (Jasp), exposed to buffer (control) or mucin, and stained for cell wall (calcofluor white) and tubulin (tubulin tracker).

(F) Percent of walled cells with nonretracted flagellum upon exposure to buffer or mucin after indicated treatment. LatB, Latrunculin B; Jasp, Jasplakinolide.

(A and F) Bold font indicates $p \leq 0.05$ by unpaired t test of independent replicates (shapes).

See also Figure S3 and Data S1.

chelators EGTA and/or BAPTA for 10 min prior to mucin exposure and observed a 23.6%–56.2% reduction in encystation ($p = 0.0002$, $p \leq 0.0001$, and $p \leq 0.0001$ for the combination; Figures 2C and S2B), suggesting that calcium flux is necessary for encystation. We next tested whether ionomycin—a calcium ionophore that transports calcium across membranes—can induce encystation. Indeed, treatment with 3 µM ionomycin induced encystation in the absence of mucin ($p = 0.0019$; Figure 2D). Further testing indicated that ionomycin does not subvert the need for adhesion (Figure 2E), indicating that once cells are adhered to a surface, calcium flux is sufficient to induce encystation. Finally, we tested whether either mucin or ionomycin could induce encystation in the nonparasitic chytrid model system *Spizellomyces punctatus* and found that they did not encyst in response to either (Figure S2C). Together, these data indicate that mucin-induced encystation is a calcium-dependent response that may be limited to *Bd*.

Cell wall assembly correlates with actin depolymerization

Fungal cell wall assembly is largely driven by enzymes that are delivered in vesicles to the plasma membrane.[25] Because zoospores have an actin cortex that may block vesicles from docking with the plasma membrane,[7] we tested whether interfering with the actin cytoskeleton would modulate mucin-induced encystation. To this end, we treated adhered zoospores with a panel of small molecules that have previously been shown to modulate actin polymerization and turnover in *Bd*,[7] as well as blebbistatin and Cytochalasin D (CytoD) that we here show alter *Bd* actin (Figures S3A and S3B), along with their vehicle controls. Although we observed no statistically significant effect of any actin inhibitor on mucin-induced encystation (Figures 3A and S3A–S3C), we found that latrunculin—a compound that sequesters actin

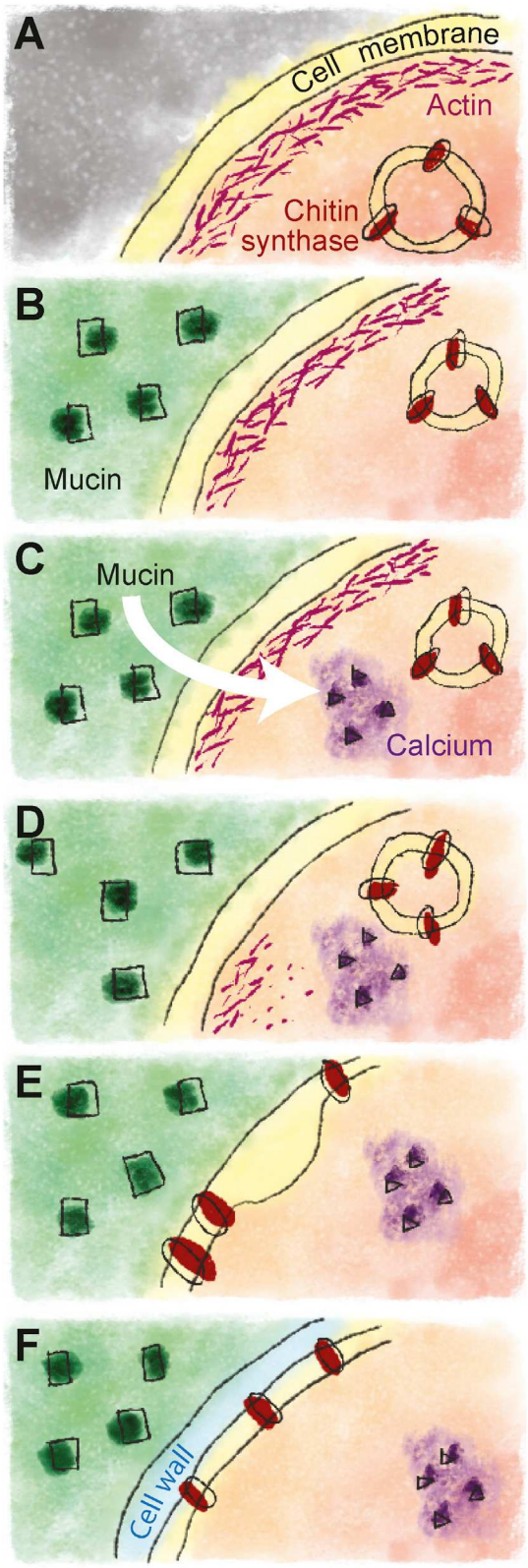

Figure 4. Model for mucin-induced encystation

(A) Based on our data and cell wall synthesis pathways in other fungal species, we propose that *Bd* zoospores contain chitin synthases and/or other cell wall synthases in intracellular vesicles that are blocked from the plasma membrane by cortical actin.

(B and C) (B) Zoospores sense when they have arrived at a host by the presence of mucin that (C) induces a transient spike in intracellular calcium.

(D and E) (D) The subsequent depolymerization of cortical actin that was previously occluding access to the plasma membrane (E) allows chitin synthase-containing vesicles to approach and fuse with the plasma membrane.

(F) The release of these enzymes then results in the rapid synthesis of cell wall material.

monomers and results in complete loss of polymerized actin in *Bd* zoospores[7]—resulted in an 16.5% ± 2.8% increase in encystation in nonmucin-treated cells ($p = 0.0040$; Figure 3A). Similarly, treatment with 10 μM jasplakinolide, a concentration that results in actin cortex reduction in *Dictyostelium*,[26] also increased encystation in nonmucin-treated cells (12.8% ± 3.3% versus 33.9% ± 0.8%, $p = 0.0033$). Together, these data indicate that actin depolymerization promotes encystation. This may be by way of depolymerizing the actin cortex to allow vesicle release, a model consistent with vesicular delivery in mammalian cells with an actin cortex similar to that of *Bd*.[7,27]

To test this hypothesis, we analyzed mucin-encysted cells treated with CytoD, an inhibitor that binds to the growing ends of actin filaments and both stabilizes and prevents further elongation. Although not statistically significant, CytoD treatment resulted in higher numbers of encysted cells in both mucin-treated and control conditions (difference of 14.5% ± 9.0%, $p = 0.1812$ and 15.6% ± 6.8%, $p = 0.0835$, respectively; Figure 3A). Interestingly, encysted cells treated with CytoD appeared to have retained cortical actin in some areas that also appeared reduced in cell wall content (Figure 3B). To quantify this relationship, we measured actin and cell wall staining intensity along the periphery of the cell and calculated the Pearson's correlation coefficient.[29] CytoD treatment resulted in a reduction in the average correlation coefficient (Figures 3B and 3C), as well as an increase in the percent of cells with a negative correlation between cortical actin and cell wall staining in mucin-treated cells (Figure 3D). Taken together, these results suggest that the reduction in cortical actin is associated with increased cell wall assembly.

During these experiments, we noted that jasplakinolide treatment resulted in cell wall assembly in cells that retained nonretracted flagella (0% ± 0% versus 46.3% ± 10.1%, $p = 0.0103$; Figure 3E). To determine if this effect is specific to jasplakinolide, we measured the number of cells with cell walls and nonretracted flagella in latrunculin-treated cells and found a similar effect (0% ± 0% versus 17.9% ± 8.0%, $p = 0.0902$; Figure 3F), suggesting that perturbation of actin dynamics can uncouple flagellar retraction from cell wall assembly during mucin-induced encystation.

Mucin as a signal that triggers encystation upon arrival at an amphibian host

Together, our data indicate that exposing *Bd* zoospores to amphibian mucus or purified mucin triggers a rapid encystation response that does not require new gene expression but does require surface adhesion. Moreover, we show that this mucin-induced encystation appears to be controlled by calcium. We also show that actin cortex disassembly is associated with cell wall accumulation. These data are consistent with the following model (Figure 4): zoospores (1) sense mucin and (2) respond

by inducing a calcium signaling cascade that results in the depolymerization of the actin cortex and (3) subsequent delivery of cell wall synthesis enzymes to the plasma membrane for (4) cell wall assembly. This model could explain how *Bd* zoospores transition from the motile dispersal form to their growth form at the appropriate time and place to increase the probability of successful host colonization.

STAR★METHODS

Detailed methods are provided in the online version of this paper and include the following:

- KEY RESOURCES TABLE
- RESOURCE AVAILABILITY
  - Lead contact
  - Materials availability
  - Data and code availability
- EXPERIMENTAL MODEL AND SUBJECT DETAILS
- METHOD DETAILS
  - Amphibian mucus collection
  - Analysis and perturbation of encystation
  - Adhesion assays
  - Small molecule inhibitors
  - Calcium signaling
  - Cell fixation and staining
  - Microscopy
- QUANTIFICATION AND STATISTICAL ANALYSIS

SUPPLEMENTAL INFORMATION

Supplemental information can be found online at https://doi.org/10.1016/j.cub.2022.04.006.

ACKNOWLEDGMENTS

We thank Fritz-Laylin lab members and Sam Lord, Madelaine Bartlett, and Meg Titus for comments on the manuscript, and Edgar Medina for *Spizellomyces* zoospores used in Figure S2C. This work was funded by the Gordon and Betty Moore Foundation (award #9337), the National Science Foundation (IOS 2143464), and a Pew Scholar award from the Pew Charitable Trusts to L.K.F.-L., who is a CIFAR fellow in the Fungal Kingdom: Threats and Opportunities program. Any use of trade, firm, or product names is for descriptive purposes only and does not imply endorsement by the U.S. Government.

AUTHOR CONTRIBUTIONS

Conceptualization, L.K.F.-L. and K.A.R.; methodology, L.K.F.-L., K.A.R., and E.H.C.G.; formal analysis, L.K.F.-L., K.A.R., and S.M.P.; investigation, K.A.R. and S.M.P.; writing – original draft, L.K.F.-L. and K.A.R.; writing – review & editing, L.K.F.-L., K.A.R., S.M.P., and E.H.C.G.; visualization: L.K.F.-L., K.A.R., and S.M.P.; supervision, L.K.F.-L.; project administration, L.K.F.-L.; funding acquisition, L.K.F.-L.

DECLARATION OF INTERESTS

The authors declare no competing interests.

Received: February 17, 2022
Revised: March 25, 2022
Accepted: April 4, 2022
Published: April 25, 2022

REFERENCES

1. Skerratt, L.F., Berger, L., Speare, R., Cashins, S., McDonald, K.R., Phillott, A.D., Hines, H.B., and Kenyon, N. (2007). Spread of Chytridiomycosis has caused the rapid global decline and extinction of frogs. EcoHealth *4*, 125.
2. Fisher, M.C., Garner, T.W.J., and Walker, S.F. (2009). Global emergence of *Batrachochytrium dendrobatidis* and amphibian chytridiomycosis in space, time, and host. Annu. Rev. Microbiol. *63*, 291–310.
3. Scheele, B.C., Pasmans, F., Skerratt, L.F., Berger, L., Martel, A., Beukema, W., Acevedo, A.A., Burrowes, P.A., Carvalho, T., Catenazzi, A., et al. (2019). Amphibian fungal panzootic causes catastrophic and ongoing loss of biodiversity. Science *363*, 1459–1463.
4. Lambert, M.R., Womack, M.C., Byrne, A.Q., Hernández-Gómez, O., Noss, C.F., Rothstein, A.P., Blackburn, D.C., Collins, J.P., Crump, M.L., Koo, M.S., et al. (2020). Comment on "Amphibian fungal panzootic causes catastrophic and ongoing loss of biodiversity". Science *367*, eaay1838.
5. Berger, L., Hyatt, A.D., Speare, R., and Longcore, J.E. (2005). Life cycle stages of the amphibian chytrid *Batrachochytrium dendrobatidis*. Dis. Aquat. Organ. *68*, 51–63.
6. Longcore, J.E., Pessier, A.P., and Nichols, D.K. (1999). *Batrachochytrium dendrobatidis* gen. et sp. nov., a chytrid pathogenic to amphibians. Mycologia *91*, 219–227.
7. Prostak, S.M., Robinson, K.A., Titus, M.A., and Fritz-Laylin, L.K. (2021). The actin networks of chytrid fungi reveal evolutionary loss of cytoskeletal complexity in the fungal kingdom. Curr. Biol. *31*, 1192–1205.e6.
8. Fritz-Laylin, L.K., Lord, S.J., and Mullins, R.D. (2017). WASP and SCAR are evolutionarily conserved in actin-filled pseudopod-based motility. J. Cell Biol. *216*, 1673–1688.
9. Piotrowski, J.S., Annis, S.L., and Longcore, J.E. (2004). Physiology of Batrachochytrium dendrobatidis, a chytrid pathogen of amphibians. Mycologia *96*, 9–15.
10. Woodhams, D.C., Alford, R.A., Briggs, C.J., Johnson, M., and Rollins-Smith, L.A. (2008). Life-history trade-offs influence disease in changing climates: strategies of an amphibian pathogen. Ecology *89*, 1627–1639.
11. Van Rooij, P., Martel, A., Haesebrouck, F., and Pasmans, F. (2015). Amphibian chytridiomycosis: a review with focus on fungus-host interactions. Vet. Res. *46*, 137.
12. Rollins-Smith, L.A. (2009). The role of amphibian antimicrobial peptides in protection of amphibians from pathogens linked to global amphibian declines. Biochim. Biophys. Acta *1788*, 1593–1599.
13. Colombo, B.M., Scalvenzi, T., Benlamara, S., and Pollet, N. (2015). Microbiota and mucosal immunity in amphibians. Front. Immunol. *6*, 111.
14. Langowski, J.K.A., Singla, S., Nyarko, A., Schipper, H., van den Berg, F.T., Kaur, S., Astley, H.C., Gussekloo, S.W.S., Dhinojwala, A., and van Leeuwen, J.L. (2019). Comparative and functional analysis of the digital mucus glands and secretions of tree frogs. Front. Zool. *16*, 19.
15. Dubaissi, E., Rousseau, K., Hughes, G.W., Ridley, C., Grencis, R.K., Roberts, I.S., and Thornton, D.J. (2018). Functional characterization of the mucus barrier on the *Xenopus tropicalis* skin surface. Proc. Natl. Acad. Sci. USA *115*, 726–731.
16. Gum, J.R., Jr. (1992). Mucin genes and the proteins they encode: structure, diversity, and regulation. Am. J. Respir. Cell Mol. Biol. *7*, 557–564.
17. Co, J.Y., Cárcamo-Oyarce, G., Billings, N., Wheeler, K.M., Grindy, S.C., Holten-Andersen, N., and Ribbeck, K. (2018). Mucins trigger dispersal of *Pseudomonas aeruginosa* biofilms. npj Biofilms Microbiomes *4*, 23.
18. Minniti, G., Rød Sandve, S., Padra, J.T., Heldal Hagen, L., Lindén, S., Pope, P.B., Ø Arntzen, M., and Vaaje-Kolstad, G. (2019). The farmed Atlantic salmon (*Salmo salar*) skin–mucus proteome and its nutrient potential for the resident bacterial community. Genes *10*, 515.
19. Muxika, A., Etxabide, A., Uranga, J., Guerrero, P., and de la Caba, K. (2017). Chitosan as a bioactive polymer: processing, properties and applications. Int. J. Biol. Macromol. *105*, 1358–1368.
20. Vancha, A.R., Govindaraju, S., Parsa, K.V.L., Jasti, M., González-García, M., and Ballestero, R.P. (2004). Use of polyethyleneimine polymer in

cell culture as attachment factor and lipofection enhancer. BMC Biotechnol. *4*, 23.

21. Verschueren, H. (1985). Interference reflection microscopy in cell biology: methodology and applications. J. Cell Sci. *75*, 279–301.
22. Rosenblum, E.B., Stajich, J.E., Maddox, N., and Eisen, M.B. (2008). Global gene expression profiles for life stages of the deadly amphibian pathogen *Batrachochytrium dendrobatidis*. Proc. Natl. Acad. Sci. USA *105*, 17034–17039.
23. Lovett, J.S. (1968). Reactivation of ribonucleic acid and protein synthesis during germination of *Blastocladiella* zoospores and the role of the ribosomal nuclear cap. J. Bacteriol. *96*, 962–969.
24. Silva, A.M., Maia, J.C., and Juliani, M.H. (1987). Changes in the pattern of protein synthesis during zoospore germination in *Blastocladiella emersonii*. J. Bacteriol. *169*, 2069–2078.
25. Gow, N.A.R., Latge, J.-P., and Munro, C.A. (2017). The fungal cell wall: structure, biosynthesis, and function. Microbiol. Spectr. *5*, https://doi.org/10.1128/microbiolspec.FUNK-0035-2016.
26. Lee, E., Shelden, E.A., and Knecht, D.A. (1998). Formation of F-actin aggregates in cells treated with actin stabilizing drugs. Cell Motil. Cytoskeleton *39*, 122–133.
27. Eitzen, G. (2003). Actin remodeling to facilitate membrane fusion. Biochim. Biophys. Acta *1641*, 175–181.
28. Kenny, M., and Schoen, I. (2021). Violin SuperPlots: visualizing replicate heterogeneity in large data sets. Mol. Biol. Cell *32*, 1333–1334.
29. Bolte, S., and Cordelières, F.P. (2006). A guided tour into subcellular colocalization analysis in light microscopy. J. Microsc. *224*, 213–232.
30. Schindelin, J., Arganda-Carreras, I., Frise, E., Kaynig, V., Longair, M., Pietzsch, T., Preibisch, S., Rueden, C., Saalfeld, S., Schmid, B., et al. (2012). Fiji: an open-source platform for biological-image analysis. Nat. Methods *9*, 676–682.
31. Prostak, S.M., and Fritz-Laylin, L.K. (2021). Laboratory maintenance of the chytrid fungus *Batrachochytrium dendrobatidis*. Curr. Protoc. *1*, e309.

STAR★METHODS

KEY RESOURCES TABLE

REAGENT or RESOURCE	SOURCE	IDENTIFIER
Biological samples		
Lithobates clamitans mucus	This study	N/A
Chemicals, peptides, and recombinant proteins		
Carbenicillin, Sodium Salt	Fisher	Cat#4800-94-6
Tetracycline HCl	Fisher	Cat#64-75-5
Concanavalin A	Sigma	Cat#C2010
Mucin from porcine stomach, type III	Sigma	Cat#M1778
Mucin from bovine submaxillary glands	Sigma	Cat#M3895
Tryptone	Sigma	Cat#T7293
D-(+)-Galactose	Sigma	Cat#G0750
Fructose	Sigma	Cat#F0127
Mannose	Sigma	Cat#M6020
N-acetylgalactosamine	Sigma	Cat#A2795
Glucosamine	Sigma	Cat#G4875
N-acetylglucosamine	Sigma	Cat#A4106
N-acetylneuraminic acid	Sigma	Cat#A0812
α-Lactose monohydrate	Sigma	Cat#L2643-500
Sucrose	Fisher	Cat#S5-500
Dextrose	Sigma	Cat#D9434-250g
Starch	Alpha Aesar	Cat#A11961
Methyl cellulose	Sigma	Cat#M7140
Glycerol	Sigma	Cat#G5516
D-sorbitol	Sigma	Cat#S1876
BSA	Fisher	Cat#BP1600-1
Polyethyleneimine	Sigma	Cat#P3143
Poly-L lysine	Sigma	Cat#P8920
Fibronectin	Sigma	Cat#F4659
Keratin	Sigma	Cat#K0253
Chitosan	Sigma	Cat#448869
Cycloheximide	Santa Cruz	Cat#SC 3508-b
Latrunculin B	Millipore	Cat#4280201MG
CK666	Calbiochem/Sigma	Cat#182515
CK689	Calbiochem/Sigma	Cat#182517
Cytochalasin D	Gibco/Life Technologies	Cat#PHZ1063
Jasplakinolide	Molecular Probes/Invitrogen	Cat#J7473
Blebbistatin	Cayman Chemical	Cat#13891
Ionomycin	Sigma	Cat#I0634
EGTA	Sigma	Cat#E4378
BAPTA	Sigma	Cat#A4926
Tubulin Tracker Deep Red	Thermo Fisher	Cat#T34077
Calcofluor white	Sigma-Aldrich	Cat#18909
Draq5	Thermo Fisher	Cat#62251
AlexaFluor 488 Phalloidin	Thermo Fisher	Cat#A12379

(*Continued on next page*)

Continued

REAGENT or RESOURCE	SOURCE	IDENTIFIER
Experimental models: Organisms/strains		
Batrachochytrium dendrobatidis strain JEL423	Longcore et al.[6]	JEL423
Spizellomyces punctatus (Koch) Barr	ATCC	117 [NG-3]
Software and algorithms		
FIJI	Schindelin et al.[30]	https://imagej.net/Fiji/Downloads
CellCounter FIJI plugin	Kurt De Vos	https://imagej.nih.gov/ij/plugins/cell-counter.html
NIS Elements w/ Advanced Research Package	Nikon	https://www.microscope.healthcare.nikon.com/products/software/nis-elements/nis-elements-advanced-research

RESOURCE AVAILABILITY

Lead contact

Further information and requests for resources and reagents should be directed to and will be fulfilled by the lead contact, Lillian Fritz-Laylin (lfritzlaylin@umass.edu).

Materials availability

This study did not generate new unique reagents

Data and code availability

- All data are available in the figures, tables, and data files associated with this manuscript.
- This study did not result in any unique code.
- Any additional information required to reanalyze the data reported in this paper is available from the lead contact upon request.

EXPERIMENTAL MODEL AND SUBJECT DETAILS

Age-matched zoospores of Batrachochytrium dendrobatidis strain JEL423 (Bd) were grown and collected as previously described.[31] Briefly, semi-synchronized cultures were grown in 1% tryptone (w/v) at 24°C in tissue culture-treated flasks (Fisher, 50-202-081). The adhered sporangia were then washed thrice with culture media, and incubated in fresh media for 2 hours 24°C. The zoospores that were released during this incubation were then collected by centrifugation at 2,500Xg. Spizellomyces punctatus (ATCC strain 48900, Sp) was grown on K1 Carb/Tet (1L; 0.6 g peptone, 0.4 g yeast extract, 1.2 g glucose, 15 g agar if plates; 50 μg/mL Carb/Tet) plates and zoospores collected by flooding each plate with 1.5 mL DS solution (50 mM KH2PO4, 50 mM K2HPO4, 50 mM (NH4)2HPO4, 50 mM MgCl2, 50 mM CaCl2). Zoospores were then transferred directly to a syringe and filtered using Whatman #1 (Fisher, 098051G).

METHOD DETAILS

Amphibian mucus collection

Northern green frog adults (Lithobates clamitans) were captured by dipnet, and transferred using new latex gloves to individual plastic bags. Individuals were measured in the bag and released, leaving behind mucus secretions on the inside surfaces of the bag. (Measurements were made for other, non-associated experiments.) Bags were transported from the field in a cooler on ice and stored at -20°C. Just before use, bags were thawed at room temperature, and mucus squeezed into the corner of each bag using a technique similar to that typically used to extrude the final remnants of toothpaste from a nearly-empty tube, and pipetted out of each corner of each bag and transferred into 1.5 mL tubes for immediate use.

Analysis and perturbation of encystation

8-well cover-glass bottom dishes (Eppendorf, 0030742036) were plasma cleaned and immediately coated with 0.5 mg/mL Concanavalin A. Synchronized zoospores were washed three times with Bonner's salts (10.27 mM NaCl, 10.06 mM KCl, 2.7 mM CaCl2 in MilliQ water), and added to individual wells. 100 μL volume of either Bonner's Salts or amphibian mucus was then added to each well while imaging.

Mucin was resuspended in Bonner's Salts for 2 hours at room temperature with shaking. Particulates were then removed by centrifugation at 15000 RCF for 2 minutes. Galactose, fructose, mannose, N-acetylgalactosamine, glucosamine, and N-acetylneuraminic acid were dissolved in Bonner's Salts at 20 mg/mL. Solutions of α-Lactose monohydrate, sucrose, dextrose, starch,

N-acetylglucosamine, and methyl cellulose were made in Bonner's Salts at 50 mg/mL. 1M solutions of Glycerol and D-Sorbitol solutions were made in Bonner's Salts. 1% BSA was made the day of the experiment in Bonner's Salts. Except when indicated, adhered synchronized zoospores in 100 μL Bonner's salts were treated with 100 μL of each solution 5 minutes before fixation. Zoospores in suspension were treated with mucin supplemented ConA, 100 μg/mL, 10 μg/mL or 1 μg/mL.

Adhesion assays

96-well plates (MatriPlate, MGB096-1-2-LG-L) were plasma cleaned and coated with one of the following: Bonner's Salts, Concanavalin A, 0.1% polyethyleneimine (w/v), 0.1% poly-L lysine (w/v), 100 μg/mL fibronectin, 1:1000 keratin, 0.05% chitosan (w/v), and 10 mg/mL porcine mucin. Wells were incubated for 1 hour and washed three times with Bonner's. Adhered synchronized Bd zoospores were washed five times with 100 μL Bonner's Salts using a 12-channel pipette. To heat kill, synchronized zoospores were placed in a 65 °C water bath for 1 minute and immediately placed on ice for 1 minute.

Small molecule inhibitors

Adhered synchronized zoospores were treated with either Bonner's Salts, DMSO or 150 μg/mL Cycloheximide (to inhibit protein translation), 1 μM Latrunculin B (to sequester actin monomers), or an equal volume of ethanol, 100 μM CK666 (to inhibit the Arp2/3 complex), 100 μM CK689 (an inactive control for CK666), 100 μM Cytochalasin D (to cap actin filaments), 10 μM Jasplakinolide (to stabilize actin filaments), 5 μM Blebbistatin (to inhibit myosin II), or equal amounts of DMSO for 10 minutes. The cells were then treated with either Bonner's Salts or mucin for 5 minutes before fixation. To test the long-term effect of Cycloheximide, synchronized zoospores were added to a 6-well TC plate (NEST, 703001). Wells were treated with concentrations of Cycloheximide suspended in 1% Tryptone for three days: 0 μg/mL, 50 μg/mL, and 150 μg/mL. On the third day, the wells were imaged using the 10X objective. To test the efficacy of phalloidin labeling on Jasplakinolide-treated cells, zoospores were treated with 10 μM Jasplakinolide before and after fixation, then labeled with phalloidin.

Calcium signaling

Bonner's Salts was used to make the solutions of 3 μM Ionomycin and DMSO carrier control. Two derivatives of Bonner's salts solutions were also used: one which replaced calcium chloride with magnesium chloride (referred to as Mg in Figure S2B) and without calcium or magnesium chloride (referred to as NDC, or No Divalent Cations, in Figure S2B). The NDC solution was used to make solutions of the following calcium chelators: 1 mM EGTA, 1 mM BAPTA, 1 mM EGTA + BAPTA, and the DMSO carrier control. From these, mucin solutions were made as described above. Adhered synchronized zoospores were pretreated with the indicated treatment for 10 minutes. The cells were then treated with the matching Bonner's Salts or mucin solution for 5 minutes before fixation.

Cell fixation and staining

Cells were fixed with 4% PFA and 50 mM sodium cacodylate, pH = 7.2 on ice for 20 minutes, then for 10 minutes at room temperature before being washed with PEM (100 mM PIPES, pH 6.9; 1 mM EGTA; 0.1 mM MgSO4). For fluorescence imaging, cells were stained with 1 μM Tubulin Tracker Deep Red, 1:1000 calcofluor white, and 5 μM Draq5 in PEM buffer for 10 minutes at room temperature. To label actin, cells were permeabilized and stained with 66 nM AlexaFluor 488 Phalloidin in 0.1% Triton-X 100-PEM buffer for 30 minutes at room temperature.

Microscopy

For live imaging, differential interference contrast (DIC) images were captured every 10 seconds using an inverted microscope (Ti-2 Eclipse; Nikon) with a 100X 1.45 NA oil objective, for a period between one minute before and nine minutes after treatment.

Fixed cells were imaged on an inverted microscope (Ti-2 Eclipse; Nikon) with either a 40X 1.45 NA oil objective or a 100X 1.45 NA oil objective and using NIS Elements software. Images were taken using both DIC microscopy and widefield fluorescence microscopy with 360 nm to visualize calcofluor white, 460 nm to visualize phalloidin, and 520 nm to visualize either Draq5 or Tubulin Tracker. IRM images were taken using a SRIC filter cube (Nikon).

QUANTIFICATION AND STATISTICAL ANALYSIS

Timelapse images were analyzed using Fiji.[30] Cells were considered pre-encysted if the cell had no flagellum and was rounded in the first image. Cells were marked as encysted on subsequent images when the flagellum had completely retracted into the cell body. Fixed images were quantified using automatic thresholding of calcofluor white or Draq5 staining in Nikon Elements or by hand using the CellCounter Fiji plugin (Kurt De Vos, https://imagej.nih.gov/ij/plugins/cell-counter.html). Unpaired t tests and ordinary one-way ANOVAs were used to assess statistical significance. The total number of cells analyzed per replicate per figure panel is available in Data S1.

Image processing and analysis for the effect of actin inhibition on *Bd* actin structures (Figure S3B) was performed using Fiji, and blind scoring using the CellCounter Fiji plugin. *Bd* zoospores were categorized based on the actin structures present in each cell, as previously defined:[7] pseudopods (actin staining 1-2 μm wide), actin spikes (actin staining <1 μm wide and ≥1μm long), cortical actin (actin staining along the edge of at least 50% of the cell), actin patches (≥10 actin spots, <1 μm in diameter), or combinations of these. Non-mucin treated cells were normalized to the DMSO-Bonner's control treatment, and mucin treated cells were normalized

to the DMSO-Mucin control treatment due to the effect of DMSO on some actin structures.[7] One-way ANOVAs were performed on these normalized values and their respective control, for three independent experiments.

Line scan analysis was performed in Fiji using the freehand selection tool and the multiplot function. The outline of control and CytoD treated cells in the presence or absence of mucin were drawn in the actin channel using a line width of three pixels. Line scans along this line were taken in both the actin and the cell wall channel, thus having two identical lines measuring the intensities from two different fluorescent signals. Each line was normalized as a percentage of the highest intensity value. Correlation analysis between the intensity values of actin and the cell wall for each cell was calculated using Pearson's Correlation Coefficient and plotted with ViolinSuperPlots[28] and compared using unpaired t tests.

Analysis on the relationship between cell wall presence and flagellar retraction was done using Fiji and the Cell Counter Plugin. Ethanol, LatB, DMSO and Jasp treated cells in the presence or absence of mucin were categorized by presence or absence of cell wall and one of four flagellar positions: in, out, partially retracted, not present. Statistical significance was assessed using unpaired t tests.